ISSN 2616-5775 Vol. 7, Issue 1: 52-58, DOI: 10.25236/AJCIS.2024.070108

Medical Images Enhancement by Integrating CLAHE with Wavelet Transform and Non-Local Means Denoising

Xiwei Liu[1,a,*], Thao Do Chi Nguyen[1,b]

[1]Mohamed Bin Zayed University of Artificial Intelligence, Masdar City, Abu Dhabi, UAE
[a]Xiwei.Liu@mbzuai.ac.ae, [b]Thao.Nguyen@mbzuai.ac.ae
[*]Corresponding author

Abstract: *Enhancement of medical images is a critical aspect in the medical field, aiming to improve the visual quality and interpretability of images for both human experts and computational analysis. This paper introduces a novel method that utilizes the strengths of Contrast Limited Adaptive Histogram Equalization (CLAHE), Wavelet Transform, and Non-Local Means (NLM) Denoising. While CLAHE enhances contrast, the Wavelet Transform provides multi-level image decomposition, and Non-Local Means Denoising effectively reduces image noise. This integrated approach overcomes the limitations of using these techniques in isolation, offering a comprehensive solution for medical image enhancement. Our method demonstrated significant improvements in image clarity and detail, particularly on FracAtlas and MURA datasets, indicating its potential for enhancing diagnostic accuracy and medical image analysis.*

Keywords: *Medical Image Enhancement, Contrast Limited Adaptive Histogram Equalization, Wavelet Transform, Non-Local Means Denoising*

1. Introduction

Medical imaging is integral to contemporary healthcare, providing essential insights for diagnosis, treatment planning, and patient monitoring. However, the effectiveness of these images is often compromised by issues such as low contrast, noise, and insufficient detail. Image enhancement, comprising various techniques to improve the visual quality or to adapt images for better analysis by humans or machines, addresses these challenges. This enhancement is a pivotal preprocessing step in image processing, especially in medical imaging, where contrast and resolution critically impact diagnostic accuracy.

Contrast enhancement, vital for better image interpretation and feature extraction, improves image quality to a more discernible level. CLAHE is a recognized method for enhancing the local contrast of images [1]. It adapts histogram equalization to smaller regions of an image, thereby avoiding noise over-amplification common with global histogram equalization techniques [2]. Despite its proficiency in enhancing local details, CLAHE may introduce artifacts and not enhance the entire image uniformly, which can be particularly noticeable in homogeneous regions [3].

Resolution indicates an image's detail-rendering capacity. Hassan Demirel et al. [4], proposed the method of image resolution enhancement using Discrete Wavelet Transform (DWT). Wavelet transforms, known for their multi-resolution capability, are widely used in image denoising and enhancement [5]. They decompose an image into frequency sub-bands, allowing for selective enhancement of certain frequency components [6]. While wavelets are effective in handling non-stationary signals in images, standard wavelet forms may not always effectively capture the intrinsic geometric structures in image data [7].

NLM denoising, introduced by Buades et al. in 2005 [8], stands out among image enhancement techniques for its utilization of information redundancy across an entire image. Unlike local denoising methods, NLM preserves edge sharpness and textural details crucial for interpreting complex images. However, its computational intensity and the tendency for over-smoothing are recognized limitations [9].

This paper proposes a medical image enhancement method combining CLAHE, NLM and DWT for bone images processing. It presents both direct and comparative analyses to illustrate the changes in

ISSN 2616-5775 Vol. 7, Issue 1: 52-58, DOI: 10.25236/AJCIS.2024.070108

images during processing. Our results, evaluated through qualitative assessments, demonstrate the effectiveness of our approach in enhancing the clarity, contrast, and overall quality of medical images.

2. Data Set

In this study, we utilized two publicly available medical imaging datasets to evaluate the proposed method. The primary dataset, FracAtlas [10], introduced in 2023, consists of 4,083 X-ray scans collected from three major hospitals in Bangladesh. These images have been manually annotated for bone fracture classification, localization, and segmentation, including 717 images with 922 instances of fractures, each provided with its own mask and bounding box annotations. Additionally, we also validate the proposed approach on the MURA dataset [11], a musculoskeletal medical imaging dataset published by Professor Andrew Ng and the ML team at Stanford, which offers an extensive collection of skeletal images.

3. Methodology

3.1. Wavelet Transform

The Wavelet Transform is a mathematical tool used for the hierarchical decomposition of images. Differing from the Fourier Transform, which only offers frequency information, wavelets are uniquely capable of providing both frequency and spatial location details. This characteristic makes them particularly suited for analyzing images with discontinuities or abrupt changes. The Wavelet Transform decomposes an image into a set of basis functions called wavelets, which are essentially scaled and translated variants of a finite-length or rapidly-decaying oscillating waveform, commonly referred to as the 'mother wavelet'. This decomposition facilitates a multi-resolution analysis, capturing an image's frequency and spatial details effectively.

The DWT for a 2D image is defined as:

$$I_{WT}(x,y) = \sum_{k,l}[LL_{k,l}\psi_{LL}(x,y;k,l) + LH_{k,l}\psi_{LH}(x,y;k,l) + HL_{k,l}\psi_{HL}(x,y;k,l) + HH_{k,l}\psi_{HH}(x,y;k,l)] \quad (1)$$

Where $I_{WT}(x,y)$ represents the wavelet transformed image, ψ_{LL}, ψ_{LH}, ψ_{HL}, ψ_{HH} are the wavelet basis functions corresponding to different frequency bands, and LL, LH, HL, HH are the wavelet coefficients.

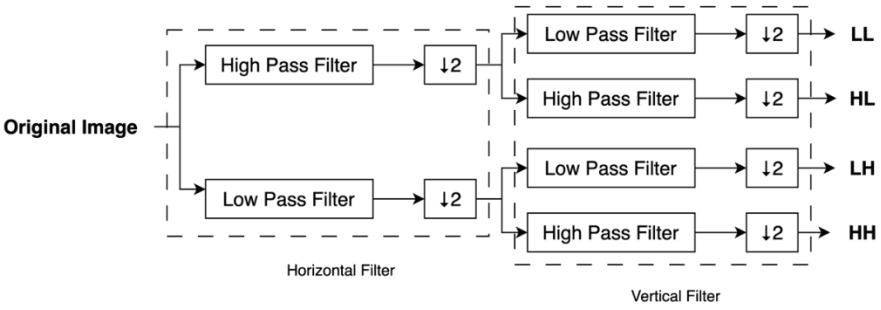

Figure 1: Decomposition of an image 2D discrete wavelet transform.

Figure 1 illustrates that an image is passed through both high-pass and low-pass filters, resulting in the decomposition of the image into high-frequency components (representing details) and low-frequency components (representing approximation) [12]. The low-frequency components reflect the overall trend of pixel values, while the details are represented in the horizontal, vertical and diagonal components. Figure 2 illustrates the first decomposition level of 2D DWT implementation on an image. At this level, the original image is decomposed into four sub-bands, each conveying frequency information in both horizontal and vertical orientations [13]. For further decomposition levels, the algorithm is recursively applied to the LL sub-band.

ISSN 2616-5775 Vol. 7, Issue 1: 52-58, DOI: 10.25236/AJCIS.2024.070108

Figure 2: Different sub-bands after first decomposition level of 2D DWT.

3.2. Non-Local Means Denoising

The Non-Local Means algorithm reduces noise by replacing each pixel's intensity with the mean intensity from similar patches elsewhere in the image [14]. Distinct from local mean filters, NLM utilizes the entire image to denoise a single pixel, thereby effectively preserving textures and edges. For a given discrete noisy image $v = \{v(i)|i \in I\}$, the estimated value $NL[v](i)$, for a pixel i, is calculated as a weighted average of all the pixels in the image.

$$NL[v](i) = \sum_{j \in I} w(i,j)v(j) \tag{2}$$

where $v(j)$ denotes the intensity of pixel j, $w(i,j)$ represents the weight based on the similarity between pixel i and j, and satisfy the usual conditions $0 \leq w(i,j) \leq 1$ and $\sum_j w(i,j) = 1$.

$$w(i,j) = \frac{1}{Z(i)} e^{-\frac{||v(N_i)-v(N_j)||^2}{h^2}} \tag{3}$$

where $Z(i)$ is the normalizing constant

$$Z(i) = \sum_j e^{-\frac{||v(N_i)-v(N_j)||^2}{h^2}} \tag{4}$$

and h serves as the filtering parameter, controlling the decay of the exponential function and consequently the decay of the weights relative to the Euclidean distances between pixels.

3.3. Contrast Limited Adaptive Histogram Equalization

Contrast Limited Adaptive Histogram Equalization is an advanced technique in image processing, primarily used for enhancing the contrast of images. Unlike traditional histogram equalization that applies a uniform transformation derived from the global contrast of the image, CLAHE operates on multiple small data regions. The main steps include the division of the input image into tiles, setting a clip limit to clip the histograms and redistributing them to other sub-blocks, and applying histogram equalization to each tile. Subsequently, the process requires interpolation of the neighboring tiles for a seamless effect [1]. The key aspect of CLAHE is its contrast limiting step, which prevents the noise amplification typically associated with standard histogram equalization [15].

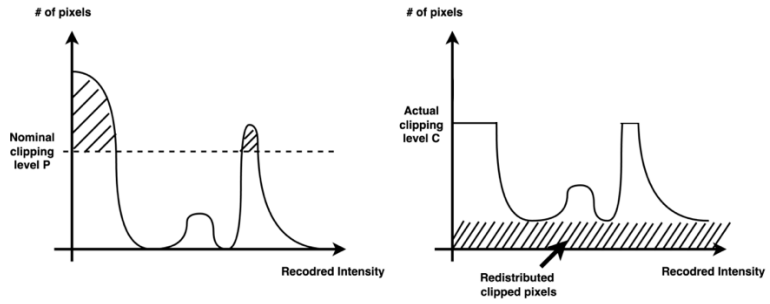

Figure 3: Concept of Contrast Limited Adaptive Histogram Equalization.

Figure 3 demonstrates the basic principle of CLAHE, it opts not to discard the part of the histogram that exceeds the clip limit but rather to equally redistribute it among all histogram bins [16]. The redistribution may cause some bins over the clip limit again, resulting in an effective clip limit that is larger than the prescribed limit and the exact value of which depends on the image. This strategy prevents

ISSN 2616-5775 Vol. 7, Issue 1: 52-58, DOI: 10.25236/AJCIS.2024.070108

any single color from aligning too abruptly to the maximum intensity, thereby maintaining a more balanced and natural visual appearance.

4. Experimental Procedure

Figure 4 shows the experimental workflow for transforming an original image into an enhanced one using the proposed method.

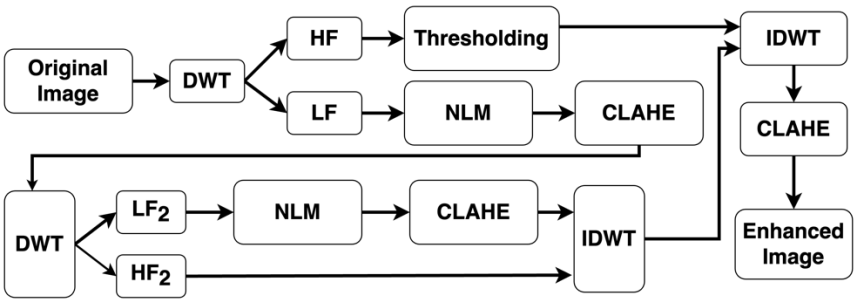

Figure 4: Experimental Flowchart.

Step One

The original image undergoes a single-level Wavelet Transform using the haar wavelet via the **dwt2()** function of MATLAB. This step decomposes the image into low-frequency (*LF*) and high-frequency (*HF*) components. The *LF* components contain the main image features, while HF components capture edges and noise. Figure 5 displays the comparison of the original image (a) and the four components (b) obtained after applying wavelet transform.

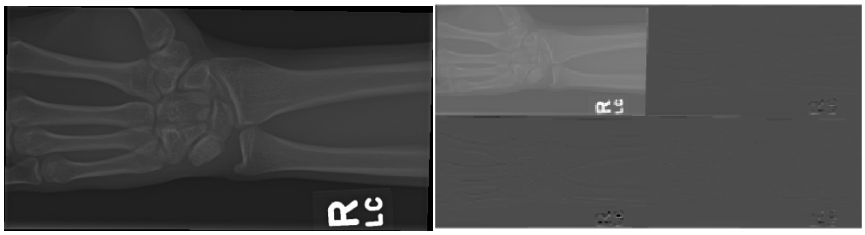

(a) Original image *(b) The wavelet transform image*

Figure 5: Comparison of the original image with the image after DWT.

Step Two

Soft threshold denoising is then applied to the *HF* components by using the **wthresh()** function. The denoising process aims to suppress noise by setting small coefficients—those that do not exceed a certain threshold—to zero, hence clearing out the unnecessary fluctuations in the wavelet coefficient matrix. Figure 6 provides an example using the *LH* component to demonstrate the effects of soft threshold denoising. The result is a smoother representation that retains important edge information while reducing the visual presence of noise, thereby enhancing the image's clarity for subsequent analysis or further processing steps.

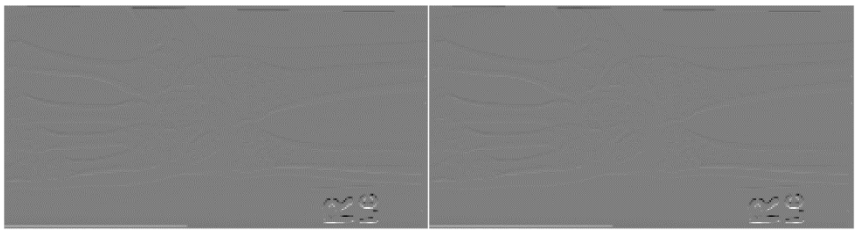

(a) LH sub-band image *(b) Soft threshold denoised LH image*

Figure 6: Comparison of the LH sub-band image before and after denoising.

Step Three

The *LF* component is refined with NLM denoising, which selectively averages the image based on

ISSN 2616-5775 Vol. 7, Issue 1: 52-58, DOI: 10.25236/AJCIS.2024.070108

the similarity of patches, effectively reducing noise without blurring the image features. It is first padded using **padarray()** function to handle the boundary effects during the denoising process. The padding replicates the border pixel intensities. A Gaussian kernel is constructed to facilitate the calculation of weighted averages of pixel intensities in the NLM step, focusing on maintaining image textures and edges. The NLM-processed LF components are subsequently enhanced by CLAHE, applied through the **adapthisteq()** function. The *clipLimit* and *tileGridSize* parameters are crucial in controlling the extent of histogram equalization, ensuring that the contrast enhancement is neither excessive nor insufficient. From Figure 7, we can clearly observe the change of LF sub-band image before and after processing.

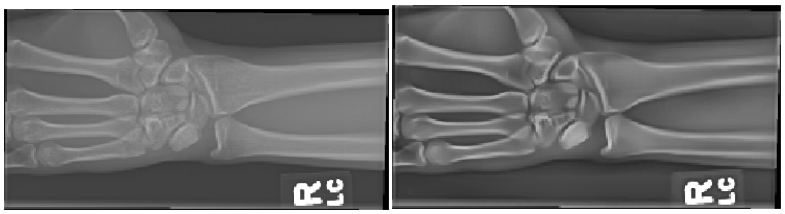

(a) Original LL sub-band image *(b) Processed LL sub-band image*

Figure 7: Comparison of the LL sub-band image before and after processing.

Step Four

This processed LF component is then decomposed again using a secondary DWT. This further breakdown produces a second set of components LF_2 and HF_2, as the second level low frequency image LF_2 shown in Figure 8 (a). Subsequently, a second application of NLM denoising coupled with CLAHE is performed on the LF_2 components. Figure 8 (b) showcases a further reduction of any residual noise and the enhancement of details, thereby enhancing and sharpening the image features.

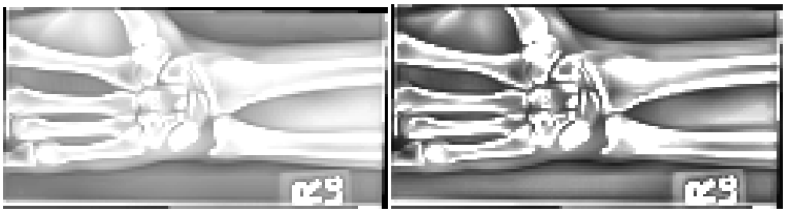

(a) Second level LF image *(b) Processed second level LF image*

Figure 8: Comparison of the second level LF image before and after processing.

Step Five

The newly processed LF_2 and HF_2 components are then recombined through Inverse Discrete Wavelet Transform (IDWT), by using **idwt2()** function, achieving a denoised version of the LF component. Figure 9 contrasts the original LL sub-band images with its enhanced counterparts after recombination.

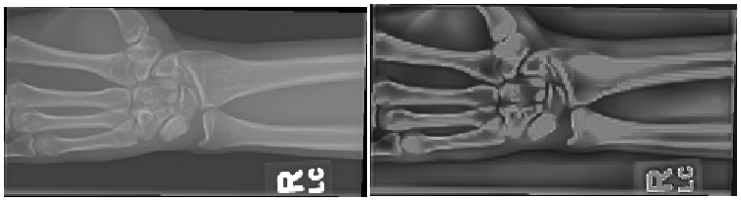

(a) Original LL sub-band image *(b) Recombined LL sub-band image*

Figure 9: Comparison of the original LL sub-band image with recombined image.

Step Six

The reconstructed LF component and denoised HF are recombined into a single image using IDWT. The IDWT reconstructs the image from its frequency components, creating an intermediate image that exhibits both the denoised features from the LF components and the preserved details from the HF components. The pre-final enhanced image is subjected to a final application of CLAHE. This last step ensures that the entire image has a uniformly improved contrast, with the visibility of features maximized across all areas. From Figure 10, we can distinctly observe that the obtained final image exhibits significant enhancements in contrast, brightness, and detail compared to the original image. This clearly demonstrates the effectiveness of the image enhancement method we have proposed.

ISSN 2616-5775 Vol. 7, Issue 1: 52-58, DOI: 10.25236/AJCIS.2024.070108

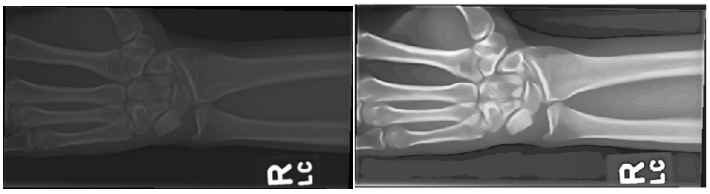

(a) Original image *(b) Final image*

Figure 10: Comparison of the original image with the final processed image.

Our experiments encompass tests on different bone sections of the MURA dataset, as well as on the FracAtlas dataset. The recorded data in Table 1 indicates significant improvements in both contrast and average gray values as a result of the processing. The average gray value of an image refers to the mean intensity of all the pixels in the grayscale image. It represents the overall brightness of the image.

Table 1: Comparison of the parameters before and after processing.

	MURA (Wrist)		MURA (Elbow)		FracAltas	
	original	processed	original	processed	original	processed
Contrast	24.208	57.774	34.913	61.733	42.938	53.253
Average Gray Value	52.915	122.497	54.620	121.820	47.065	107.178

5. Conclusion

In this paper we presented an innovative approach to medical image enhancement, integrating CLAHE, Wavelet Transform, and NLM Denoising. DWT assists in decomposing image components into sub-bands for better analysis. CLAHE is specially applied to low frequency to enhance the local contrast of the images, and NLM denoising effectively addresses the noise amplification caused by CLAHE, while preserving essential details. The proposed method is proved effective in addressing common issues in medical imaging, such as low contrast, noise, and lack of detail, significantly improving image quality. Our results, validated on the FracAtlas and MURA datasets, demonstrate marked enhancements in clarity, contrast, and overall image quality.

References

[1] S.M. Pizer, E.P. Amburn, J.D. Austin, R. Cromartie, A. Geselowitz, T. Greer, B. ter Haar Romeny, J.B. Zimmerman, and K. Zuiderveld, Adaptive histogram equalization and its variations, Computer vision, graphics, and image processing 39 (1987), pp. 355–368.

[2] K. Zuiderveld, Contrast limited adaptive histogram equalization, Graphics gems (1994), pp. 474–485.

[3] A.M. Reza, Realization of the contrast limited adaptive histogram equalization (clahe) for real-time image enhancement, Journal of VLSI signal processing systems for signal, image and video technology 38 (2004), pp. 35–44.

[4] H. Demirel and G. Anbarjafari, Discrete wavelet transform-based satellite image resolution enhancement, IEEE transactions on geoscience and remote sensing 49 (2011), pp. 1997–2004.

[5] S.G. Mallat, A theory for multiresolution signal decomposition: the wavelet representation, IEEE transactions on pattern analysis and machine intelligence 11 (1989), pp. 674–693.

[6] I. Daubechies, Ten lectures on wavelets, SIAM, 1992.

[7] J. Portilla, V. Strela, M.J. Wainwright, and E.P. Simoncelli, Image denoising using scale mixtures of gaussians in the wavelet domain, IEEE Transactions on Image processing 12 (2003), pp. 1338–1351.

[8] A. Buades, B. Coll, and J.M. Morel, A non-local algorithm for image denoising, in 2005 IEEE computer society conference on computer vision and pattern recognition (CVPR'05), Vol. 2. Ieee, 2005, pp. 60–65.

[9] K. Dabov, A. Foi, V. Katkovnik, and K. Egiazarian, Image denoising by sparse 3-d transform-domain collaborative filtering, IEEE Transactions on image processing 16 (2007), pp. 2080–2095.

[10] I. Abedeen, M.A. Rahman, F.Z. Prottyasha, T. Ahmed, T.M. Chowdhury, and S. Shatabda, Fracatlas: A dataset for fracture classification, localization and segmentation of musculoskeletal radiographs, Scientific Data 10 (2023), p. 521.

[11] P. Rajpurkar, J. Irvin, A. Bagul, D. Ding, T. Duan, H. Mehta, B. Yang, K. Zhu, D. Laird, R.L. Ball, et al., Mura: Large dataset for abnormality detection in musculoskeletal radiographs, arXiv preprint arXiv:1712.06957 (2017).

[12] R.C. Gonzalez, Digital image processing, Pearson education india, 2009.

ISSN 2616-5775 Vol. 7, Issue 1: 52-58, DOI: 10.25236/AJCIS.2024.070108

[13] A.K. Jain, Fundamentals of digital image processing, Prentice-Hall, Inc., 1989.
[14] A. Buades, B. Coll, and J.M. Morel, A non-local algorithm for image denoising, in 2005 IEEE Computer Society Conference on Computer Vision and Pattern Recognition (CVPR'05), Vol. 2. 2005, pp. 60–65 vol. 2.
[15] D. Martinez, Online adaptive histogram equalization, in Neural Networks for Signal Processing VIII. Proceedings of the 1998 IEEE Signal Processing Society Workshop (Cat. No. 98TH8378). IEEE, 1998, pp. 531–538.
[16] G.R. Vidhya and H. Ramesh, Effectiveness of contrast limited adaptive histogram equalization technique on multispectral satellite imagery, in Proceedings of the International Conference on Video and Image Processing. 2017, pp. 234–239.